Supplement of Geosci. Model Dev., 15, 6709–6745, 2022
https://doi.org/10.5194/gmd-15-6709-2022-supplement

Geoscientific Model Development
Open Access
EGU

Supplement of

LPJ-GUESS/LSMv1.0: a next-generation land surface model with high ecological realism

David Martín Belda et al.

Correspondence to: David Martín Belda (david.belda@kit.edu)

	LAI (obs)	LAI (mod)	PAR (LPJ-G)	PAR (LPJ-G/LSM)	% Change
AU-Emr	0.7	0.6	426	651	53.4
ES-Amo	-	2.1	708	928	32.1
AU-DaP	1.5	7.9	1839	1959	6.5
AU-Stp	0.5	2.2	607	774	28.6
CG-Tch	2.0	11.6	1925	1994	3.6
PA-SPs	5.4	11.1	1986	2076	4.5
AU-DaS	1.5	3.0	2150	2450	14.1
AU-Dry	1.2	2.6	1837	2183	18.9
SD-Dem	0.9	1.3	456	664	45.6
AU-Ade	1.1	3.0	2157	2460	14.1
AU-Gin	0.9	1.5	1553	2010	29.5
AU-How	1.5	3.4	2403	2634	9.7
AU-RDF	1.6	3.2	2283	2527	10.7
AU-Rob	4.3	4.9	2378	2430	2.2
BR-Sa1	6.5	5.7	2463	2470	0.3
BR-Sa3	6.5	4.7	2102	2169	3.2
GF-Guy	5.9	5.2	2377	2419	1.8
GH-Ank	-	5.1	1843	1879	1.9
MY-PSO	6.5	5.3	2385	2415	1.3
PA-SPn	2.9	4.9	2079	2129	2.4
ZM-Mon	1.6	2.4	1314	1635	25.0

Table S1: Comparison of PAR absorbed by the vegetation, calculated using the new radiative transfer scheme and the PAR absorption scheme in standard LPJ-GUESS. Data are from the CLM/Med simulations described in the paper. PAR values are averages over the measurement period of the simulations, in MJ/year/m^2. The percent change is relative to the standard LPJ-GUESS run.

1 Differences in PAR absorption between LPJ-GUESS and LPJ-GUESS/LSM

Table S1 shows a comparison of average PAR absorption per unit LAI calculated by the new radiative transfer scheme and the PAR absorption algorithm in stadard LPJ-GUESS. The calculations were made in the CLM/Med simulation, i.e., PAR absorption is calculated with both schemes in the same modeled areas for the purpose of this comparison. In general, the new radiative transfer calculates higher absorbed PAR values than standard LPJ-GUESS at sites with low modeled LAI values, while both calculations yield similar results at sites with high LAI values. This behaviour can be understood by examining PAR absorption by individual cohorts. Figure S1 shows PAR absorption by the vegetation over 60 years during the spinup period at BR-Sa1, starting after a disturbance. Three tree cohorts (0, 1 and 2) and a grass individual (4) establish. Initially, grass has a high LAI, but, as trees grow and the canopy thickens, the grass LAI declines (panels *c* and *d*). Calculated tree PAR absorption per leaf area is initially similar for both schemes (panel *a*), but as cohort 0 grows it shadows cohorts 1 and 2. The new radiative transfer scheme calculates lower PAR values for these two cohorts, but since their leaf area index is also declining, this does not contribute substantially to the overall difference, which is small and dominated by cohort 0 (panel *b*).

Figure S2 shows the same comparison for a patch at AU-Gin. In this case, the tree cohorts have a lower leaf area index, so their leaves receive, on average,

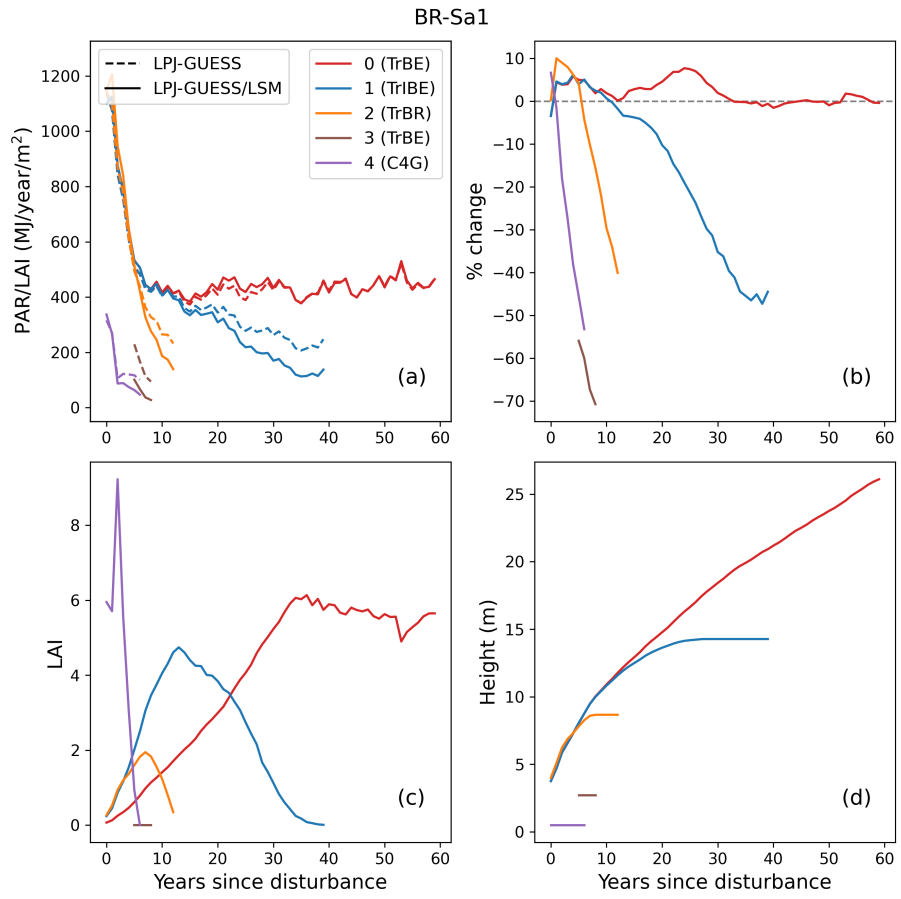

Figure S1: Comparison of PAR absorbed by the cohorts in a patch at BR-Sa1, calculated using the new radiative transfer scheme and the standard LPJ-GUESS PAR absorption scheme. *(a):* Annual absorbed PAR per leaf area; *(b):* Percent change in PAR absorption relative to standard LPJ-GUESS; *(c):* LAI; *(d):* Cohort height.

more direct sunlight than in the case of a thicker canopy. The new radiative scheme calculates higher values of absorbed PAR for these cohorts (panels *a* and *b*), and this feature dominates the overall difference between the two schemes in this site.

2 Spinup information

In a standard LPJ-GUESS simulation the 500-year spinup process proceeds as follows: the first 100 years, the model runs without nitrogen uptake to allow build up of soil nitrogen pools. All vegetation in the patch is then reset, and plant nitrogen uptake is turned on. Between years 140 and 220, information on the rates of change of C and N pools is collected. This information is then used to calculate carbon and nitrogen steady-state pool sizes analitically, assuming

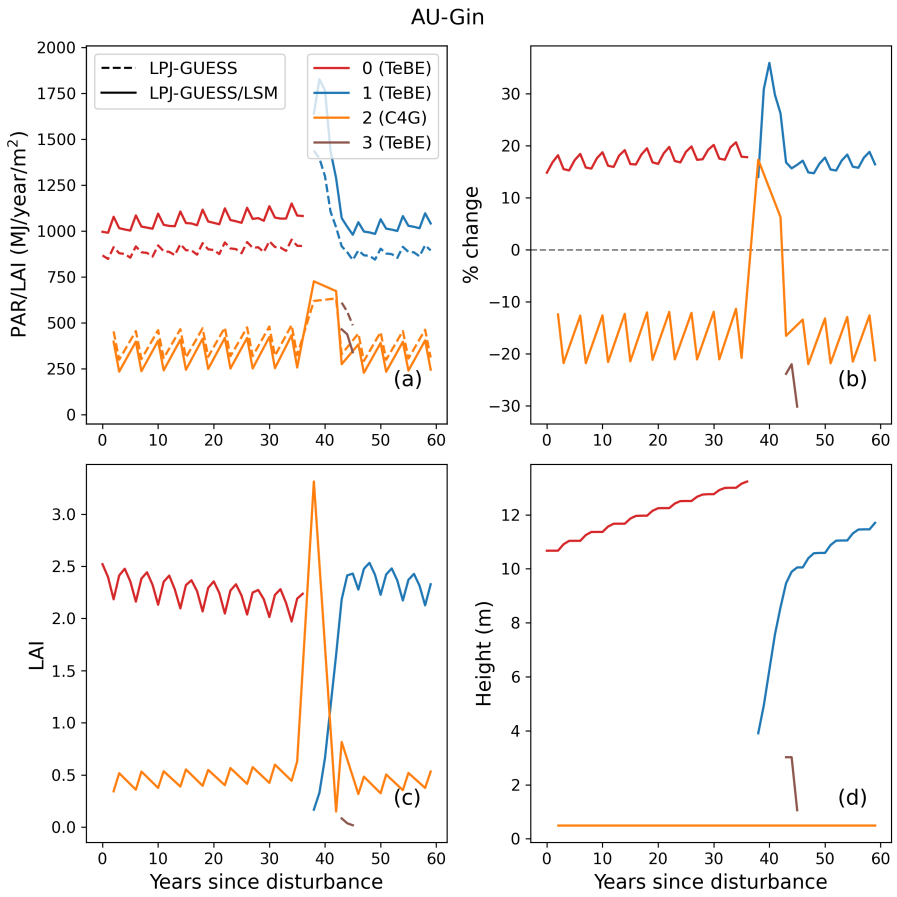

Figure S2: Comparison of PAR absorbed by the cohorts in a patch at BR-Sa1, calculated using the new radiative transfer scheme and the standard LPJ-GUESS PAR absorption scheme. *(a):* Annual absorbed PAR per leaf area; *(b):* Percent change in PAR absorption relative to standard LPJ-GUESS; *(c):* LAI; *(d):* Cohort height.

an equilibration time of 40000 years for the soil organic matter pools. The model then runs for another 280 years, a period considered long enough for the vegetation C and N pools to reach steady state.

In general, the steady-state size of the carbon and nitrogen pools is determined by the balance between the rate of carbon input to the system (NPP) and the turnover rates of the soil organic matter pools. The LSM implementation changes the physical environment at which these processes take place in the model. Calculating photosynthesis rates at the newly simulated leaf temperature can lead to higher or lower carbon assimilation, depending on the PFT's optimal photosynthetic temperature range. It can also boost productivity by mitigating the effect of N limitation (see paper, Section 4.2). Soil organic matter decomposition is affected by soil temperature and humidity; higher (lower) temperatures and humidities lead to higher (lower) turnover rates. Table S2 shows

	BB					Med				
	NPP	Temp	AWC	Soil C	Soil N	NPP	Temp	AWC	Soil C	Soil N
AU-Emr	-66.7	13.1	-30.0	-74.1	-74.1	-68.7	14.4	-49.6	-75.3	-75.3
ES-Amo	6.1	3.3	-11.6	-12.9	-12.9	0.6	3.7	-29.9	-12.9	-12.7
AU-DaP	1.8	4.5	46.2	-12.8	-10.2	25.5	4.4	19.8	21.7	25.7
AU-Stp	-42.8	8.5	-24.1	-50.5	-50.4	-23.0	9.0	-37.0	-33.6	-33.4
CG-Tch	87.6	2.5	51.5	6.8	9.2	92.0	1.8	52.1	10.4	12.9
PA-SPs	34.7	1.2	6.7	22.2	24.3	38.9	1.2	3.5	27.2	29.4
AU-DaS	-11.8	0.9	42.1	-0.9	3.5	-6.5	1.7	16.5	15.9	21.3
AU-Dry	-7.1	3.8	47.1	-2.0	1.0	1.4	3.3	11.8	4.5	6.5
SD-Dem	-13.1	-0.4	85.0	-45.9	-47.2	34.8	-0.3	-0.0	43.6	46.6
AU-Ade	-13.4	0.8	34.9	8.1	15.6	-8.7	0.8	16.6	21.4	29.5
AU-Gin	0.6	6.2	56.3	-32.7	-32.3	-9.1	6.0	25.7	-25.3	-23.6
AU-How	-13.8	-0.5	37.9	2.9	10.2	-10.6	-0.0	20.8	18.6	27.8
AU-RDF	4.6	3.3	45.4	15.0	19.9	12.0	3.6	21.0	28.7	33.1
AU-Rob	4.4	1.1	18.3	-6.4	-6.2	3.3	1.1	13.0	-2.1	-1.4
BR-Sa1	-25.2	-0.5	8.1	-16.0	-15.3	-20.5	-0.6	5.7	-14.2	-13.3
BR-Sa3	-11.1	-2.4	5.6	-8.7	-8.4	-6.2	-2.5	-3.2	-6.5	-6.3
GF-Guy	-14.6	0.3	9.9	-14.7	-14.5	-11.3	0.6	6.0	-12.6	-12.3
GH-Ank	-23.9	-0.3	13.3	-15.6	-13.4	-18.8	-0.7	11.4	-13.8	-11.5
MY-PSO	-30.1	0.3	59.2	-43.1	-42.6	-23.2	0.5	54.4	-37.5	-37.4
PA-SPn	-15.8	0.6	8.5	-20.6	-18.5	-12.1	0.7	5.5	-16.0	-13.6
ZM-Mon	-1.6	3.9	68.9	-18.1	-12.9	-3.8	1.8	39.5	-20.1	-15.3

Table S2: Percent change in steady-state NPP, average soil temperature over the top 50 cm of soil, average water content over the top 50 cm of soil, soil carbon content, and soil nitrogen content, relative to standard LPJ-GUESS. Steady state values are taken as the average of the last 100 years of spinup.

a comparison of these factors in LSM and standard LPJ-GUESS simulations for all the sites considered in this study.

We show two examples of the build-up of the soil organic matter pools at BR-Sa1 (Fig. S3) and SD-Dem (Fig. S4), for the standard LPJ-GUESS, the CLM/BB, and the CLM/Med runs. At BR-Sa1 in the BB simulation, equilibrium NPP is lower than in standard LPJ-GUESS by $\sim$ 25% (Table S2). Soil temperature is similar to standard LPJ-GUESS, but soil moisture is $\sim 8\%$ larger. This leads to lower equilibrium soil carbon ($\sim -16\%$) and nitrogen ($\sim -15\%$) content. The CLM/Med simulation behaves similarly at this site (and at most forest sites).

At SD-Dem the BB and Med simulations show very different behaviours. In the BB simulation, NPP is lower than in LPJ-GUESS, while the higher stomatal resistance given by the Ball-Berry scheme (see paper, Fig. 3) causes higher soil moisture content. This leads to lower equilibrium soil organic matter content values (a $\sim$ 46% decrease compared to standard LPJ-GUESS). In the Med simulation, equilibrium NPP is substantially higher than in the standard LPJ-GUESS run, while lower soil moisture retention leads to slower decomposition rates, resulting in soil organic matter pools $\sim$ 44% larger than in standard LPJ-GUESS.

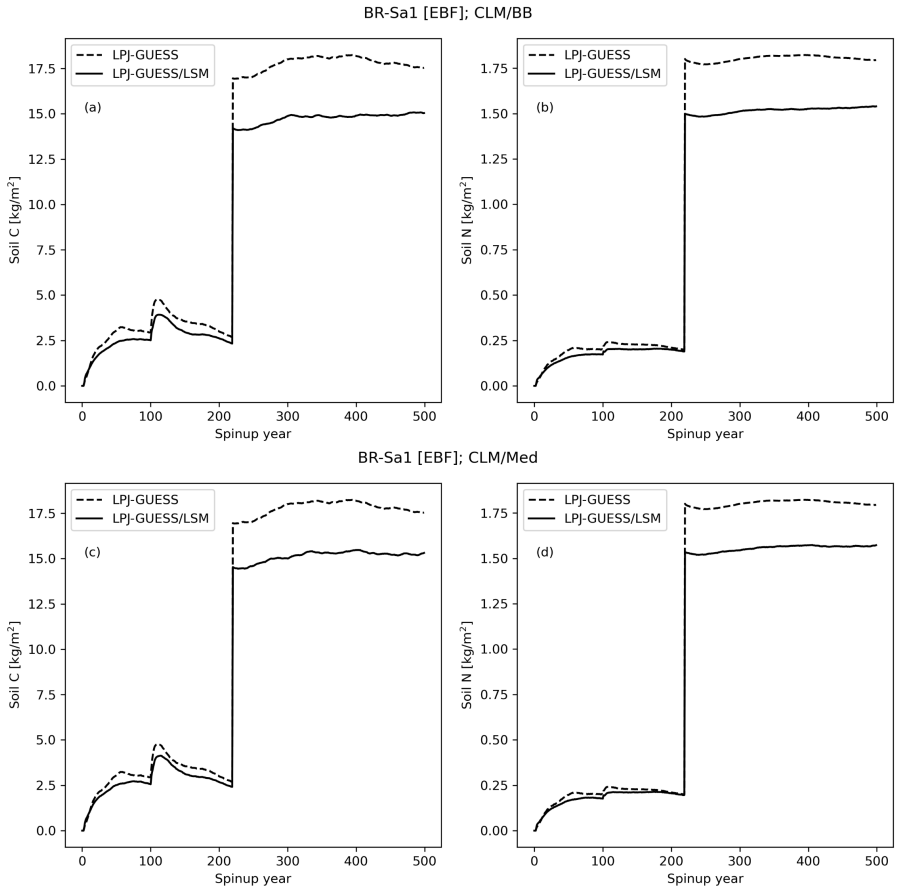

Figure S3: Comparison of the build up of carbon and nitrogen pools in the CLM/BB *(a) and (b)* and the CLM/Med *(c) and (d)* simulations with standard LPJ-GUESS, at BR-Sa1.

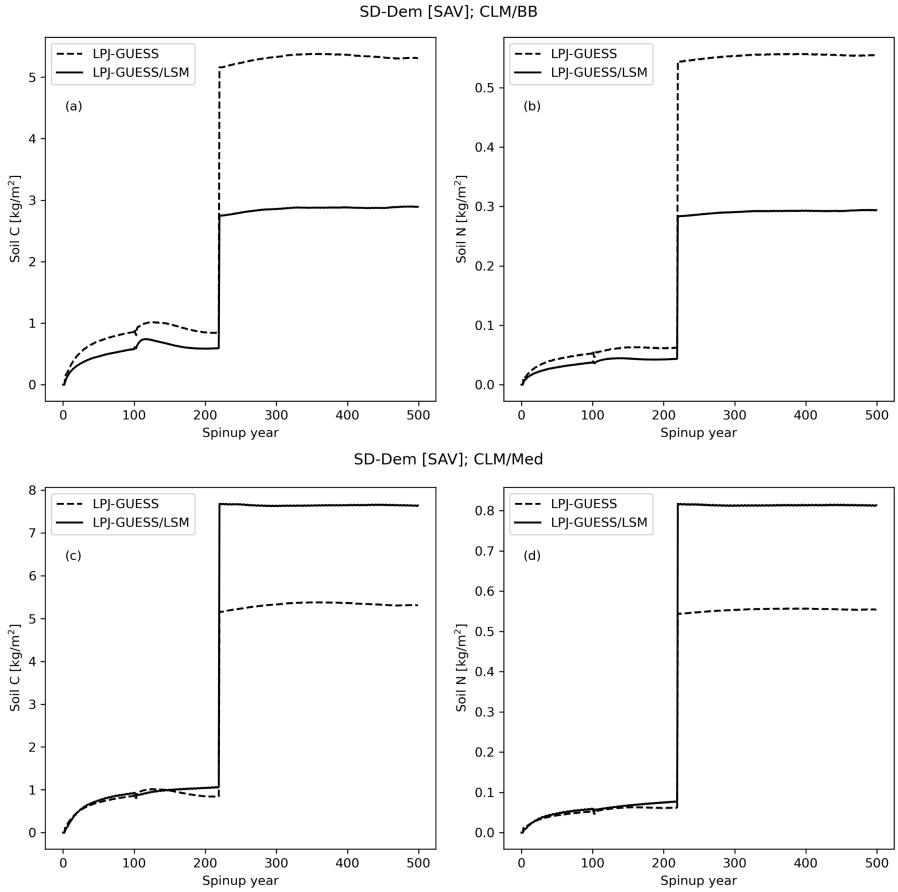

Figure S4: Comparison of the build up of carbon and nitrogen pools in the CLM/BB *(a) and (b)* and the CLM/Med *(c) and (d)* simulations with standard LPJ-GUESS, at SD-Dem.